International Core Journal of Engineering Volume 9 Issue 7, 2023
ISSN: 2414-1895 DOI: 10.6919/ICJE.202307_9(7).0008

Study on Nitrate Nitrogen based on Ultraviolet Visible Absorption Spectroscopy

Li Zhang, Yitong Yin, and Jinrui Zeng

Chongqing Key Laboratory of Optoelectronic Information Sensing and Transmission Technology, School of Optoelectronic Engineering, Chongqing University of Posts and Telecommunications, Chongqing 400065, China

Abstract

In order to improve the accuracy of nitrate nitrogen detection, this paper proposes a method for rapid determination of nitrate nitrogen in water based on UV visible absorption spectroscopy. The experimental subjects were the absorption spectra of sodium nitrate standard solution with a concentration range of 0.1~20mg L-1. The principal component analysis method PCA (Principal Component Analysis) was used to find the appropriate number of principal components. Use Support Vector Regression (SVR) to fit the absorbance and sample concentration at characteristic wavelengths, and establish a regression model for nitrate nitrogen. The root mean square error (RMSE) is used as the evaluation indicator for the model. The experiment found that the RMSE of the mixed prediction model established using PCA-SVR modeling method was 0.00779mg L-1, and its modeling effect was better than SPA-SVR, achieving rapid and accurate measurement of nitrate nitrogen.

Keywords

Nitrate Nitrogen; Absorption Spectrum; Water Quality Detecting.

1. Introduction

With the development of society and the acceleration of urbanization, a large amount of nitrogen-containing wastewater is directly discharged into the water. Excessive nitrogen content in water bodies can lead to the proliferation of microorganisms, vigorous growth of plankton, and eutrophication of water bodies[1]. After being absorbed by the human body, NO3-N in water will be reduced to NO2-N, and a large amount of NO2-N will reduce the oxygen transport capacity of the blood, causing harm to the human body[2]. In order to prevent further aggravation of nitrogen pollution, it is necessary to quickly detect nitrate nitrogen in water bodies.

At present, the detection methods of nitrate nitrogen mainly include phenol disulfonic acid spectrophotometry, ultraviolet spectrophotometry, ion selective electrode method, ion chromatography, gas phase molecular absorption spectrometry[3], etc. However, the above methods are difficult to meet the requirements of practical application due to many interfering substances, poor selectivity, harsh experimental conditions, long analysis time, and the need to consume chemical reagents.

UV absorption spectroscopy is a method for qualitative, quantitative, or structural analysis of substances based on spectral data in the 200-800 nm spectral region. It has the advantages of sample free processing, pollution-free, simple operation, and real-time[4]. It has been widely used in fields such as environmental monitoring, pollutant analysis, drug testing, and food safety[5]. K. Mikael et al.[6] used diode arrays to obtain the UV visible absorption spectra of urban domestic sewage, and analyzed them using multivariate data analysis methods. This method can also simultaneously

ISSN: 2414-1895 DOI: 10.6919/ICJE.202307_9(7).0008

measure other components such as TP, TN, ammonia nitrogen in water. O. Zielinski et al.[7] used a high-resolution ultraviolet spectrophotometer to measure the concentration of nitrate at the tidal inlet, applied it to the high turbidity seawater domain, and proposed an improved algorithm for high turbidity water samples. S. Uusheimo et al.[8] studied the effect of TOC on nitrate and nitrite using two types of UV visible sensors, 5 mm and 35 mm. Using laboratory measurements as a reference, they established calibration curves for nitrate and nitrite, and corrected the effect of TOC.

2. Experiment

2.1 Experimental Device

An experimental platform for ultraviolet visible absorption spectroscopy was established, mainly including light sources, sample cells, fiber optic collimators, spectrometers, and computers, as shown in Figure 1. The deuterium halide lamp (Wenyi Optoelectronics, DH-mini compact type) is used as the light source for the UV visible absorption spectrum. The light emitted by the light source is coupled through optical fibers, and then emitted to the sample pool through an optical fiber collimator (Wenyi Optoelectronics, 74UV). The generated output light is collected through the collimator, and received by a spectrometer (Shared Optics, PG2000 pro) through optical fibers. Finally, the collected data is stored, processed, and modeled on the computer side.

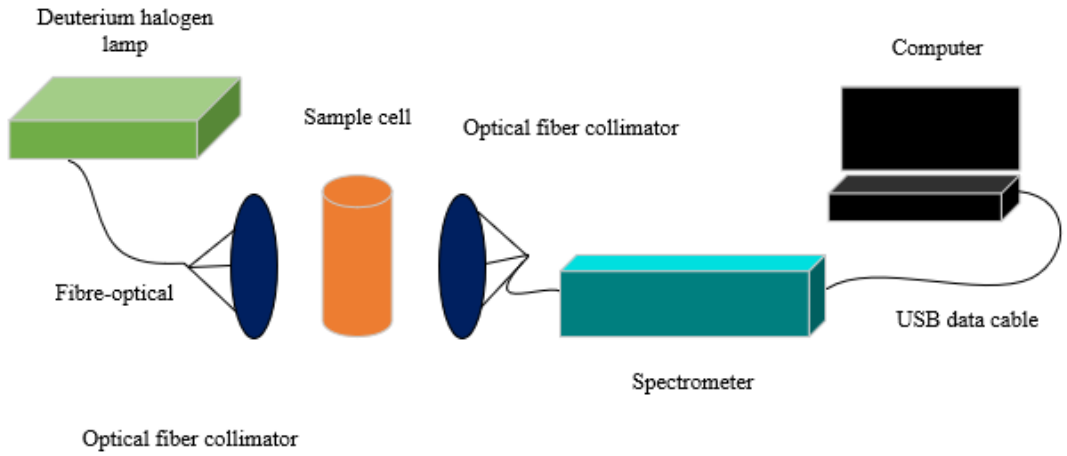

Figure 1. Experimental device diagram

2.2 Sample Preparation

This article uses the standard substance for nitrate nitrogen solution (1000 mg·L-1, Northern Weiye) as an experimental sample, and prepares a series of concentration gradient solutions through gradual dilution. The concentration range is 0.1~20 mg·L-1, and in the range of 0.1~2 mg·L-1, the concentration gradient is 0.1 mg·L-1; In the range of 2-5 mg·L-1, the concentration gradient is 0.25 mg·L-1; In the range of 5 to 20 mg·L-1, the concentration gradient is 1 mg·L-1. Dilute the original standard solution step by step with deionized water and a 1 mL rubber tipped dropper to prepare solutions of different concentrations. Divide them into multiple 250mL experimental bottles, label them accordingly, and write down the corresponding concentration and preparation time. The experimental platform used was a laboratory built experimental setup system, with a spectrometer integration time of 45 ms, an average of 10 times, and a smoothness of 3. Firstly, it is necessary to collect the absorbance of deionized water as a blank control. After introducing deionized water, the dark background is deducted first, and then the absorption spectrum under the bright background is collected. Finally, the absorption spectrum is saved and changed to the corresponding name. After the collection is completed, the deionized water will be discharged, and the standard solution will be introduced twice before being discharged to moisten the sampling tube and reduce experimental

ISSN: 2414-1895 DOI: 10.6919/ICJE.202307_9(7).0008

errors. After the third introduction of the standard solution, the absorption spectrum of the nitrate nitrogen solution can be collected according to the steps of collecting deionized water. It is important to collect the nitrate nitrogen solution in order of concentration from low to high as much as possible, in order to observe changes in the spectrum and detect errors in a timely manner.

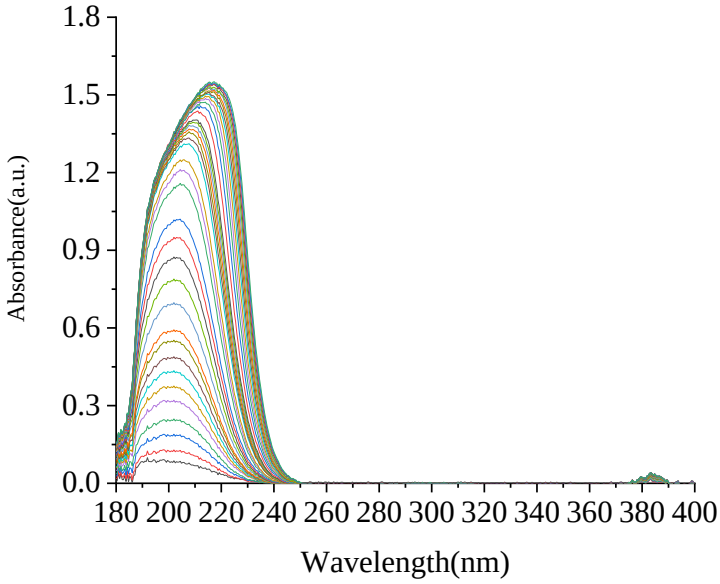

Figure 2. Ultraviolet absorption spectrogram of nitrate nitrogen standard solution

From the above figure, it can be seen that nitrate nitrogen has two absorption peaks in the purple light region. The first absorption peak is the main absorption peak, with a wavelength range of 190-240 nm. The second absorption peak is the secondary absorption peak, with a wavelength range of 375-390 nm. On the left side of the main absorption peak, some spectra overlap severely. In the main absorption peak range, as the concentration increases, its absorbance increases, and the increase amplitude first increases and then decreases. When the concentration of nitrate nitrogen increases to a certain concentration, its spectrum begins to overlap, indicating that at this concentration, the absorbance of nitrate nitrogen solution begins to saturate. In the sub absorption peak range, the absorbance value is small, indicating that the nitrate nitrogen solution contains less spectral information in this band range.

3. Establishing a Mixed Prediction Model

The collected high-dimensional raw spectral data contains a lot of redundant information, so effective feature extraction is necessary. This section used two feature extraction methods, PCA and SPA, to extract features from the original spectral data of nitrate nitrogen. Then, SVR was used to establish a regression model. Finally, the modeling effects of these two different feature extraction methods were compared.

3.1 Comparison of Different Feature Extraction Methods

1) Principal Component Analysis

When processing high-dimensional data, PCA is a common dimensionality reduction method, and when using it, it is necessary to select the appropriate number of principal components in order to optimize the dimensionality reduction effect. This section compares the RMSE of the test set under different number of principal components to find the appropriate number of principal components, as shown in Figure 3.

ISSN: 2414-1895 DOI: 10.6919/ICJE.202307_9(7).0008

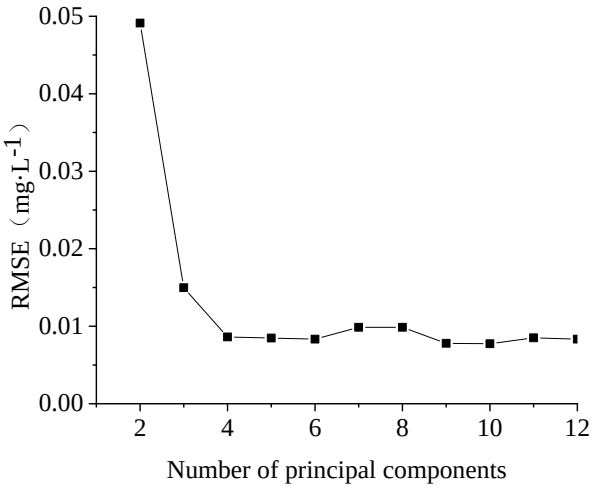

Figure 3. Change curve of root mean square error of test set decision under PCA algorithm

Divide the samples into training and testing sets in a 7:3 ratio. From Figure 3, it can be seen that as the number of principal components increases, the root mean square error (RMSE) of the testing set shows a decreasing trend. When the number of principal components increases from 2 to 3, the amplitude of change between the two is the largest, and then the amplitude of change becomes smaller and smaller until it stabilizes and remains basically unchanged. As shown in the figure, when the number of principal components is 9, the RMSE is the smallest, and the model performs the best. At this time, the RMSE of the model test set is 0.00779 mg L-1. As shown in Figure 3-5, the comparison between the true and predicted values of the test set when the number of main components is 9.

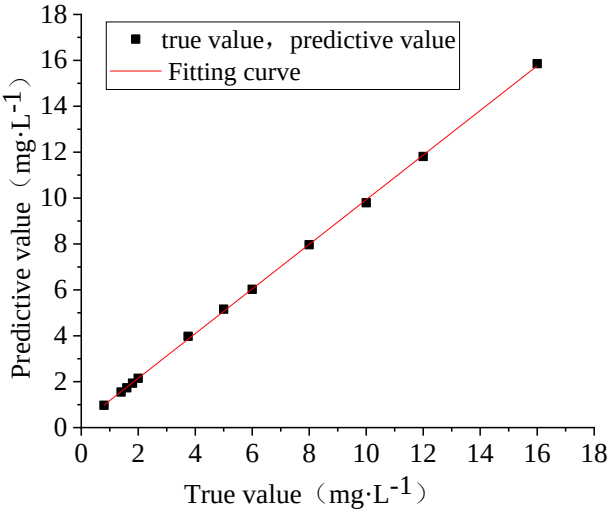

Figure 4. Comparison between true and predicted values of test set samples under PCA algorithm

2) Continuous projection algorithm

SPA is another common feature extraction method, which, unlike PCA, requires determining the number of feature wavelength points extracted from the original spectral data. If the number of feature wavelength points extracted is too small, the original data will lose some useful information after dimensionality reduction, leading to a decrease in the accuracy of the final model prediction; However,

ISSN: 2414-1895 DOI: 10.6919/ICJE.202307_9(7).0008

the number of extracted feature wavelength points should not be too large, otherwise the modeling data will also contain useless information, which also affects the performance of the model. Therefore, the optimal number of feature wavelengths to be extracted is determined by the curve of RMSE changing with the number of feature wavelengths extracted by SPA. The specific test set RMSE changes with the number of feature wavelengths are shown in Figures 5, 6.

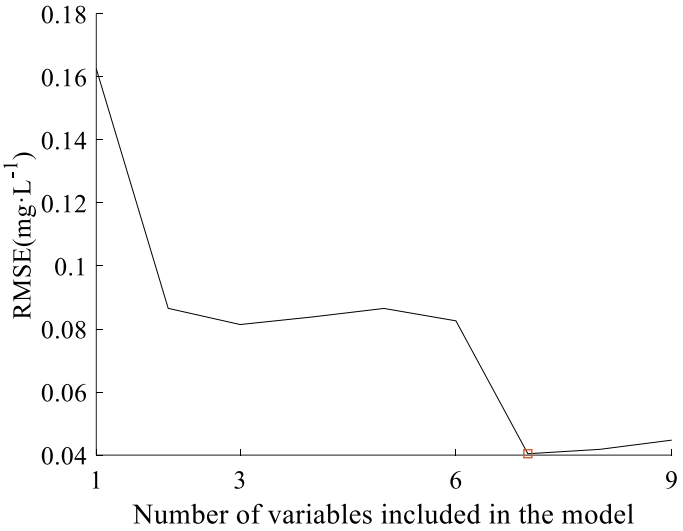

Figure 5. Change curve of root mean square error of test set under SPA algorithm

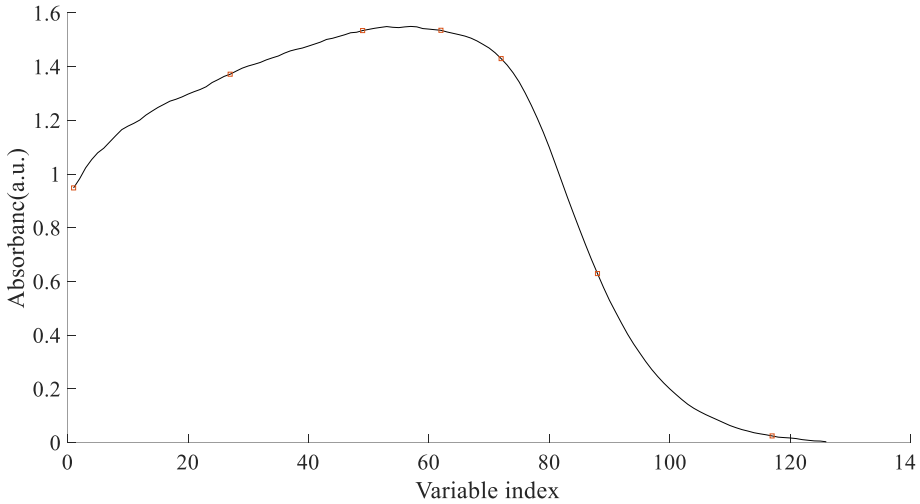

Figure 6. Selected Characteristic Wavelengths for SPA

From Figure 5, it can be seen that when the number of extracted feature wavelengths increases from 1 to 2, the RMSE of the test set decreases significantly. When the number of extracted feature wavelengths is between 2 and 6, the RMSE does not change significantly. However, as the number of extracted feature wavelengths continues to increase, the RMSE continues to decrease significantly, and reaches its minimum value of 0.040431 when the number is 7. When the number of extracted feature wavelengths continues to increase from 7, RMSE actually increases, indicating that the subsequent addition of feature wavelength points contains useless information, leading to a decrease in the performance of the model. When the number of extracted feature wavelengths is 7, the fitting diagram of the true and predicted values of the test set is shown in Figure 7.

ISSN: 2414-1895 DOI: 10.6919/ICJE.202307_9(7).0008

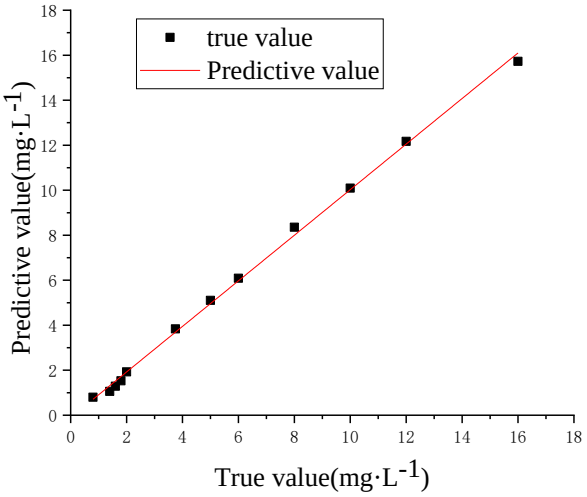

Figure 7. Comparison between the real value and the predicted value of the test set sample under the SPA algorithm

3.2 Comparison of Modeling Effects

As shown in Table 1, the comparison of the modeling effects of two feature extraction methods under optimal conditions is presented.

Table 1. Comparison of modeling results

Feature extraction method	Parameter/(mg·L^{-1})	Test set RMSE/(mg·L^{-1})	Test set RMSE (mg L^{-1})
PCA	Number of principal components=9	SVR	0.00779
SPA	Number of characteristic wavelengths=7	SVR	0.040431

From Table 1, it can be seen that the RMSE obtained when using PCA for feature extraction is smaller, indicating that the modeling effect when using PCA for feature extraction is better than that when using SPA for feature extraction. As shown in Table 2, the true values, predicted values, and their errors of each sample are tested under the prediction model established for feature extraction.

Table 2. Predicted value of nitrate nitrogen concentration PCA-SVR mixed model

Sample number	Predicted value/(mg·L^{-1})	True value/(mg·L^{-1})	Relative error/%
1	1.80	1.8349	1.93
2	6.00	6.0235	0.39
3	1.40	1.4846	6.04
4	5.00	5.0586	1.17
5	10.00	9.7967	2.03
6	1.60	1.6232	1.45
7	8.00	7.9636	0.45
8	3.75	3.8114	1.63
9	16.00	15.8533	0.92
10	12.00	11.8096	1.59
11	0.80	0.8549	6.86
12	2.00	2.0511	2.55

ISSN: 2414-1895 DOI: 10.6919/ICJE.202307_9(7).0008

From the table, it can be seen that when the sample concentration is below 2 mg · L-1, there are two samples with relative errors of 6.04% and 6.86%, not exceeding 10%, respectively. The relative errors at other concentrations are all within 5%, indicating that the modeling method used in this article is correct and has high applicability, which can complete the detection of nitrate nitrogen.

Acknowledgments

National Natural Science Foundation of China (61805030), Chongqing Basic and Frontier Technology Research Project (cstc2020jcyj-msxmX0147), Chongqing Education Commission Science and Technology Project (KJQN202000640, KJZD-M202200602).

References

[1] Lu Haifeng, Peng Meng, Zhang Guangming, et al. Biokinetic and biotransformation of nitrogen during photosynthetic bacteria wastewater treatment[J]. Environmental Technology, 2018, 41(15): 1888-1895.

[2] Agusta H., Kartika J., Sari K. Nitrate concentration and accumulation on vegetables related to altitude and sunlight intensity[J]. IOP Conference Series: Earth and Environmental Science, 2021, 896(1): 012052.

[3] Zhuang Yanhua, Wen Weijia, Ruan Shuhe, et al. Real-time measurement of total nitrogen for agricultural runoff based on multiparameter sensors and intelligent algorithms[J]. Water Research, 2022, 210: 117992.

[4] L Pigani, S.G. Vasile, G.Foca, et al. Talanta, 2017, 178: 178-187.

[5] Li Guan, Yifei Tong, Jingwei Li, et al. RSC Advances, 2019, 9, 11296-11304.

[6] Mikael K., Bo K., Olsson R. Determination of nitrate in municipal waste water by UV spectroscopy[J]. Analytica Chimica Acta, 1995, 312(1): 107-113.

[7] Zielinski O., Voβ D., Saworski B, et al. Computation of nitrate concentrations in turbid coastal waters using an in situ ultraviolet spectrophotometer[J]. Journal of Sea Research, 2011, 65(4): 456-460.

[8] Uusheimo S., Tulonen T., Arvola L., et al. Organic carbon causes interference with nitrate and nitrite measurements by UV/Vis spectrometers: the importance of local calibration[J]. Environmental Monitoring and Assessment, 2017, 189(7): 357.